Exp Brain Res (1993) 96:443-456

Experimental Brain Research

Modularity and parallel processing in the oculomotor integrator

J. Douglas Crawford*, Tutis Vilis

Departments of Physiology and Ophthalmology, University of Western Ontario, London, Ontario, Canada N6A 5C1

Received: 27 January 1993 / Accepted: 25 June 1993

Abstract. The neural signals that hold eye position originate in a brainstem structure called the *neural integrator*, so-called because it is thought to compute these position signals using a process equivalent to mathematical integration. Most previous experiments have assumed that the neural integrator reacts to damage like a single mathematical integrator: the eye is expected to drift towards a unique resting point at a simple exponential rate dependent on current eye position. Physiologically, this would require a neural network with uniformly distributed internal connections. However, Cannon et al. (1983) proposed a more robust *modular* internal configuration, with dense local connections and sparse remote connections, computationally equivalent to a parallel array of independent sub-integrators. Damage to some sub-integrators would not affect function in the others, so that part of the position signal would remain intact, and a more complex pattern of drift would result. We evaluated this parallel integrator hypothesis by recording three-dimensional eye positions in the light and dark from five alert monkeys with partial neural integrator failure. Our previous study showed that injection of the inhibitory γ aminobutyric acid agonist muscimol into the mesencephalic interstitial nucleus of Cajal (INC) causes almost complete failure of the integrators for vertical and torsional eye position after ~ 30 min. This study examines the more modest initial effects. Several aspects of the initial vertical drift could not be accounted for by the single integrator scheme. First, the eye did not initially drift towards a single resting position; rapid but brief drift was observed towards multiple resting positions. With time after the muscimol injection, this range of stable eye positions progressively narrowed until it eventually approximated a single point. Second, the drift had multiple time constants. Third, multiple regression analysis revealed a significant correlation between drift rate and magnitude of the previous saccade, in addition to a correlation between drift rate and position. This saccade dependence enabled animals to stabilize gaze by making a series of saccades to the same target, each with less post-saccadic drift than its predecessor. These observations were predicted and explained by a model in which each of several parallel integrators generated a fraction of the eye-position command. Drift was simulated by setting the internal gain of some integrators at one (perfect integration), others at slightly less than one (imperfect integration), and the remainder at zero (no integration), as expected during partial damage to an anatomically modular network. These results support the previous suggestion that internal connections within the neural integrator network are restricted to local modules. The advantages of this modular configuration are a relative immunity to random local computational errors and partial conservation of function after damage. Similar computational advantages may be an important consequence of the modular patterns of connectivity observed throughout the brain.

Key words: Oculomotor – Interstitial nucleus of Cajal – Integrator – Parallel processing – Monkey

Introduction

In the last few years much attention has been focused on the principle of parallel distributed processing in the brain, mainly with reference to connectionist models (Crick 1989; Arnold and Robinson 1991). These models emphasize the importance of lateral connections between parallel channels. Modular connectivity, e.g. the columns of sensory cortex (Mountcastle 1957; Hubel and Weisel 1959), is one basic pattern that has been observed throughout the brain without any clear rationale for its significance (Purves et al. 1992). This pattern is not as obvious in some motor systems, but has been theoretically proposed for a simple and well-defined motor operator, the oculomotor integrator (Cannon et al. 1983). The

* *Present address:* Montreal Neurological Institute, 3801 University Street, Montreal, Quebec, Canada H3A 2B4

Correspondence to: T. Vilis

purpose of the present study was to test this hypothesis experimentally and explore its implications.

David A. Robinson was the first to suggest the existence of a neural integrator in the oculomotor system. He noted that the primary commands for eye movement resemble eye velocity signals and so proposed that the neural eye-position signal is derived from the former signals by a process equivalent to mathematical integration (Robinson 1968). The positional drift that results from damage to such an integrator would account for the commonly observed clinical disorder called gaze-evoked nystagmus (Leigh and Zee 1991). The experimental search for this neural integrator amassed favourable evidence. Stimulation of the paramedian pontine reticular formation induced constant-velocity horizontal eye movements that held their final position, suggesting that the induced activity had been integrated (Cohen and Komatsuzaki 1972), while lesions of the cerebellum gave rise to eye position drift consistent with imperfect integration (Carpenter 1972, Robinson 1974). This search culminated in the discovery of a small area in the nucleus prepositus hypoglossi and medial vestibular nucleus that is essential for maintenance of horizontal position of both eyes during all conjugate movements, i.e. the horizontal integrator (Cannon and Robinson 1987; Cheron and Godaux 1987).

Where then are the integrators for the other two dimensions of eye position? The mesencephalic interstitial nucleus of Cajal (INC) appears to possess circuits essential for the vertical eye position integrator. The role of the INC in producing the vertical eye position signal is suggested by: (1) a correlation between neural activity in the INC and vertical eye position (King et al. 1981; Fukushima et al 1990), (2) a reduction of gain of the vestibulo-ocular reflex after inactivating the INC (Anderson et al. 1979); (3) failure in holding vertical eye positions during INC inactivation (King and Leigh 1982; Fukushima 1987; Crawford et al. 1991).

The third dimension of eye rotation is torsion, which we define as rotation of the eye about a head-fixed axis approximately orthogonal to the face. Clockwise and counterclockwise rotations are described from the subject's point of view. Injection of inhibitory γ-aminobutyric acid (GABA) agonist muscimol into the INC produced a profound deficit not only in vertical eye position holding, but also in holding torsion (Crawford et al. 1991). Stimulation of the right INC produced clockwise constant-velocity eye rotations that held, while left INC stimulations produced similar counterclockwise rotations. This, in combination with single unit recordings (Fukushima et al. 1990), suggests that the INC is organized with clockwise-up and clockwise-down eye rotations represented on the right side, and counterclockwise-up and counterclockwise-down on the left (Crawford et al. 1991). Thus, the INC appears to be the principle centre for both the vertical and torsional oculomotor integrators.

Neural integration is an important concept in oculomotor physiology with possible implications for general postural control, and has therefore inspired a number of theoretical examinations (Rosen 1972; Kamath and Keller 1976; Cannon et al. 1983; Galiana and Outerbridge 1984; Tweed and Vilis 1987; Arnold and Robinson 1991). At the core of most integrator models is a simple positive feedback loop that retains a constant level of neural activity when input is zero. Damage to such an integrator would produce a simple position-dependent exponential drift of the eye towards a unique resting position, with a time constant that is inversely proportional to the amount of damage. Cannon et al. (1983) pointed out that in these models, integrator function is very sensitive to minute errors in feedback gain that result from random computational errors or tissue damage. For example, reduction of excitatory feedback gain by only 0.4% would decrease the time constant of integrator leak from a behaviourally determined normal value of 20–25 s to 1.2 s, i.e. the position signal would decrease by 63% in this time. Such an arrangement is clearly not robust.

The solution to this problem clearly involves increasing the number of neurons in the network. However, while it is obvious that integration is not achieved by a single neuron, it may not be as obvious that a multi-neuron network can be computationally equivalent to a single-neuron model. A network with uniformly distributed connections suffers from a similar lack of robustness (Arnold and Robinson 1991) because damage to any synapse affects overall gain in the distributed feedback loop. Cannon et al. (1983) addressed this problem in an integrator network model that used parallel units that indirectly excited themselves though mutually inhibitory lateral connections (Cannon et al. 1983). The key point for this discussion is that the lateral connections were organized so that connections were dense between neighbouring units, but sparse between distant units. Taken to an extreme, such a pattern would result in a network of parallel and independent sub-integrators. This model was much more robust. During simulations of localized damage to the network the resultant drift was initially rapid, then stabilized within a second, essentially holding at a slightly less eccentric position that was maintained by the remaining intact integrator circuits (Cannon et al. 1983). These intact circuits could eventually be recalibrated to compensate for those that were damaged. However, experimental investigations have continued to assign single time constants and resting positions to post-saccadic drift, as if it were produced by a single leaky integrator (Cannon and Robinson 1987; Cheron and Godaux 1987; Fukushima 1987; Crawford et al. 1991; Straube et al. 1991).

The purpose of the present investigation was *not* to develop a new model of the oculomotor integrator, but rather to test the important principle outlined above. The question is whether the oculomotor velocity-to-position transformation utilizes a uniform distribution of lateral connections (Arnold and Robinson 1991), equivalent to a single integrator, or a modular pattern (Cannon et al. 1983), equivalent to multiple parallel independent integrators. Whereas our previous study emphasized complete failure of the torsional and vertical oculomotor integrators $\sim$30 min after injection of muscimol into the INC (Crawford et al. 1991), the present study reports the

more modest initial effects and the time course of their progression. The observed ocular drift is then compared in the Discussion section to drift simulated by two simple models of the saccade generator. These used either a single integrator to simulate a fully distributed network or an array of parallel integrators to simulate a compartmentalized network.

In brief, simulated damage to a single integrator gives three predictions: (1) eye position will settle towards a unique resting point; (2) the rate of eye position drift is a direct function of current eye position; (3) this position dependence gives the drift a simple exponential time course that can be described by a single time constant. In contrast, with parallel independent integrators, some sub-integrators could be completely inactivated while others would remain intact, and the other modules would have intermediate deficits. Therefore, three different predictions result: (1) eye position could settle at multiple resting positions retained by position signals from the intact sub-integrators; (2) since a constant fraction (proportionate to the fraction of damaged sub-integrators) of the neural movement command will not be correctly integrated, large saccades will produce more post-saccadic drift than small saccades, i.e. the drift should be saccade dependent; (3) since activity in differentially damaged sub-integrators will leak to zero at different rates, the resultant drift will have multiple time constants. The data exhibited all of the latter three characteristics, strongly suggesting that a modular form of parallel processing is utilized in the mechanism of neural integration.

Materials and methods

Measurement of three-dimensional (3D) eye positions

Five *Macaca fascicularis* (coded MAR, BAR, LAR, CAS, ART) were prepared for chronic behavioural experiments, each monkey undergoing surgery under aseptic conditions and pentobarbital anaesthesia. During surgery a skull cap composed of dental acrylic was fastened to the animal's head, and two enamelled copper search coils of 5 mm diameter were implanted in one eye for measurement of 3D eye position. Both coils were positioned nasally, one inferior and one superior. The method used did not require that the coils be aligned orthogonally to each other (Tweed et al. 1990). The leads were extended temporally beneath the conjunctiva and then subcutaneously to sockets secured on the cap. In two of the animals (CAS and ART), coils were implanted in both eyes. During experiments, the head of the alert monkey was immobilized by fixing the skull cap near the centre of three orthogonal magnetic fields. These fields were in phase, but operated at different frequencies (62.5, 125, and 250 kHz). The resultant coil signals were digitized by a computer at a sampling frequency of 100 Hz.

In all animals, coil signals were recorded while the animals spontaneously made saccades between visual targets in the light, placed so as to reveal the animal's full range of attainable eye positions. In two animals (BAR and LAR), data were also recorded while animals spontaneously made saccades in the dark. Control data were collected at the beginning of each experiment for comparison.

Since the INC is thought to control both vertical and torsional eye movements, a 3D representation of eye position was required. Therefore, the computer was used to convert coil signals into eye position quaternions, both on-line and off, using a method described previously (Tweed et al. 1990). Quaternions are composed of a scalar part q_0, and a vector part $\mathbf{q}$. It is the vector part that is used for representation of data. The vector part has three components along torsional, horizontal and vertical axes fixed relative to the head. To be more precise, the direction of vector $\mathbf{q}$ gives the axis of the rotation that would take the eye from a reference position to the current position, and the length of $\mathbf{q}$ is proportional to the magnitude of this rotation. The quaternion vector is related to the axis and magnitude of such a rotation as follows

$$\mathbf{q} = \mathbf{n} \sin(\alpha/2) \quad (1)$$

The angle α is the magnitude of the rotation and $\mathbf{n}$ is a 3-dimensional unit vector parallel to the axis of rotation (Tweed and Vilis 1987). At reference position α = zero and thus $\mathbf{q}$ = zero. This reference position was recorded while the monkey looked in the direction of the forward-pointing magnetic field. Detailed discussions of eye position quaternion recording and mathematics are available elsewhere (Westheimer 1957; Tweed and Vilis 1987; Tweed et al. 1990; Crawford and Vilis 1991). In this paper the vector components of quaternions will simply be referred to as the torsional, vertical, and horizontal components of position.

With the head upright and still, eye positions normally conform to Listing's law (Helmholtz 1925). This law states that any arbitrarily chosen reference eye position is associated with a particular head-fixed plane, such that the eye only assumes positions that can be reached from this reference position about an axis in that plane. Furthermore, there is one special reference position, *primary position*, for which the gaze direction is orthogonal to its associated plane. This is called *Listing's plane*. By defining ocular torsion as rotation about the head-fixed axis orthogonal to Listing's plane, one can restate Listing's law very simply: the eye only assumes positions with a zero torsional component (Westheimer 1957).

Quaternions vectors computed from raw coil signals were originally, by default, in a coordinate system defined by the magnetic field directions. All data were then rotated into Listing's coordinates (Tweed et al. 1990). By this we mean that the vertical and horizontal coordinates were aligned in Listing's plane, and the torsional coordinate was parallel with the primary gaze direction. This primary gaze direction, as originally defined by Helmholtz (1925), varies with respect to anatomical landmarks (Tweed et al. 1990; Crawford and Vilis 1991). Thus, primary gaze is not necessarily equivalent to a central or straight ahead direction, contrary to popular usage of the term. The advantage of representing quaternion vectors in Listing's coordinates is that it gives an unambiguous and physiologically meaningful depiction of vertical/horizontal movement within Listing's plane of normal saccadic eye positions and torsional movement orthogonal to this plane (Crawford and Vilis 1991, 1992).

Invasive neurophysiological procedures

Before initiating experiments, a stainless steel recording chamber was mounted stereotaxically over a trephine hole in the skull centred at 8 mm anterior and 0 mm lateral, directly over the oculomotor nucleus (Shantha et al. 1968). During experiments a hydraulic microdrive attached to the recording chamber was used to advance electrodes and cannulas into the midbrain. After the midbrain oculomotor region had been located, one electrode penetration was generally made per day. The regions of oculomotor activity along this penetration were examined by means of single unit recording, microstimulation, and pharmacological inactivation techniques. In this fashion each animal's midbrain oculomotor region was systematically explored with an orderly grid of electrode penetrations over a period of several months.

Monopolar tungsten electrodes (Frederick Haer, 4 MΩ) were used to record from units and to stimulate. The electrode was inserted in an insulated guide cannula which was manually advanced into the brain stem to within 5 mm of the selected oculomotor region. Subsequently the electrode was hydraulically advanced by

up to 10 mm from the guide cannula. Units were identified by comparing their discharge patterns with eye movements and positions. Afterwards the same electrode was used to microstimulate the region at vertical intervals of 0.5 mm by means of monophasic cathodal square pulses delivered at 20 μA and 200 Hz for durations of 300 to 600 ms.

Finally, the electrode was pulled out of its guide tube without otherwise disturbing the tube or the microdrive, and a 30-gauge cannula was then inserted into the guide tube and lowered to a depth determined during the unit recording and stimulation phases, usually just above the selected oculomotor region. A Hamilton syringe was used to deliver 0.3 μl of a 0.05% muscimol solution. Muscimol has a powerful inhibitory effect on neurons that posses GABA receptors. Thus, muscimol should inhibit action potential generation in local cell bodies without disrupting fibres of passage. For comparison, 0.3 μl of a 2% GABA solution was also injected into two animals. Eye-movement recordings commenced immediately after the injection and continued for 30 min or more. Afterwards the animal was allowed a 48-h recovery period, and then experiments were repeated at an adjacent brain site displaced lateral-medial or rostral-caudal by 1 mm.

When the midbrain oculomotor region had been thoroughly explored, the animals were deeply anaes-thetized with pentobarbital, and then electrolytic lesions (1.5 mA DC anodal current for 15 s) were made at a reference microdrive coordinate. Immediately afterwards animals were given a lethal dose of anaesthetic and perfused with an intra-aortic injection of formalin. The brains were removed, sliced into 100-μm sections and stained with thionin. The resulting slides were compared to a stereotaxic atlas of the monkey brain (Shantha et al. 1968) to confirm the anatomical locations of the recording sites.

Identification of the INC region

Single unit recordings identified a region in the midbrain with neural activity correlated to vertical eye position that corresponded to the expected stereotaxic location of the INC. Neurons that increased their activity either during upward or downward eye positions were intermingled on each side of the brain, and most of these also showed a burst of activity during saccades in these directions, as previously described for the INC region (King et al. 1981; Fukushima et al. 1990). The anterior-laterally adjacent saccade-related burst region, which was completely inactive during fixation, corresponded to the rostral interstitial nucleus of the medial longitudinal fasciculus (riMLF) (King and Fuchs 1979; Crawford and Vilis 1992) There was less distinction between these putative INC neurons and a posterior-medially adjacent group of putative 3rd cranial nucleus motoneurons. However, electrical stimulation of the putative INC neurons elicited conjugate torsional eye movements which held their final position (Crawford et al. 1991), whereas stimulation of the more posterior putative motoneurons produced disconjugate eye rotations in various directions that did not hold their final positions (Crawford and Vilis 1992). The initial effect of muscimol injection into the anterior burst region was a conjugate deficit in saccade velocities (Crawford and Vilis 1992). The initial effect of injection into the posterior putative motoneurons was a disconjugate restriction in the position range and saccade velocities. The initial effect of injection into the intervening region, believed to be the INC, was the distinctive conjugate post-saccadic drift described below in the Results. This functional identification of the mesencephalic oculomotor structures was consistent with the known anatomy of the region, as confirmed by our histological procedures.

Muscimol was injected unilaterally into the INC 14, 8, 3, 3, and 10 times in animals BAR, CAS, MAR, LAR, and ART, respectively. Of these experiments, 6 in BAR and 1 in LAR were performed in the dark as well as light. This was in addition to 1, 1, and 2 bilateral injections in animals BAR, CAS and ART respectively. In every case, injection resulted in a deficit in maintaining vertical and torsional position of both eyes that ranged from mild to extreme, with little horizontal drift (Crawford et al. 1991). Injection of muscimol directly into the INC region produced immediate oculomotor deficits, whereas it took approximately 30 min for a prominent oculomotor deficit to appear after an injection 1 mm lateral to the INC region. This suggested that during this period muscimol inactivated oculomotor units within a sphere with a radius of slightly more than 1 mm. Injection of GABA directly into the INC produced the same initial effects as muscimol, but recovery was observed within 10 min. The oculomotor effects of muscimol took at least 30 min to peak, and judging by other observed deficits (e.g. contralateral tilting of the head), recovery required several hours.

Results

Progressive decrement in the range of stable eye positions

During integrator failure, the direction of position drift should depend on initial post-saccadic position (a function of the saccade generator) and also on the position where the eye comes to rest (a function of neural integrator output). Figure 1 gives a torsional versus vertical plot

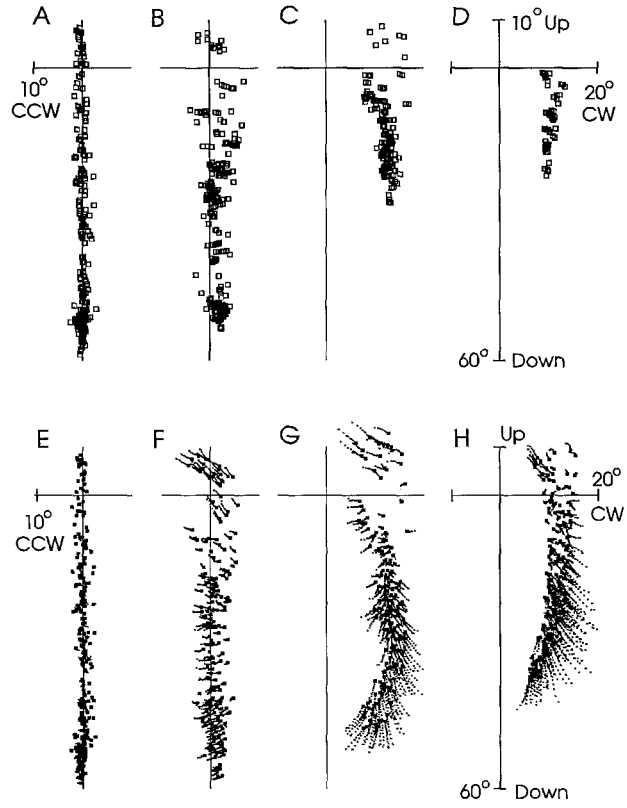

Fig. 1A–H. Time course of torsional and vertical eye position holding and drift after injection of muscimol directly into the left interstitial nucleus of Cajal. **A–D** Eye positions during which eye speed was less than 2.5°/s. **A** before injection, **(B)** 0–2 min, **(C)** 14 min, and **(D)** 23 min after injection. **E–H** The first 100 ms of eye positions are shown after each of several hundred randomly directed saccades, computed from the same data as **A–D**. Larger data points demarcate the last position of each 100-ms sequence. Torsional position is plotted as a function of vertical position in Listing's coordinates, i.e. the vertical axis is embedded in Listing's plane. The origin is the primary position as defined by Listing's law and is usually located high in the oculomotor range of *Macaca fascicularis* (Crawford and Vilis 1991, 1992). Animal: ART

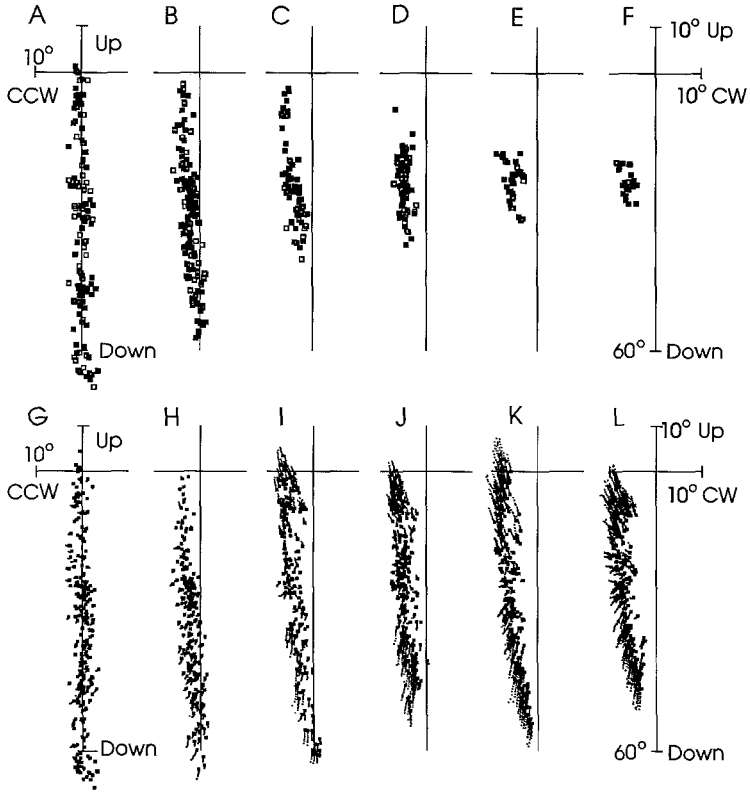

Fig. 2A–L. Time course of torsional and vertical eye position holding and drift after injection of muscimol adjacent to the anterior-lateral pole of the right interstitial nucleus of Cajal. **A–F** Eye positions during which eye speed was less than 2.5°/s, **A** before injection, and **(B)** 9 min, **(C)** 19 min, **(D)** 21 min, **(E)** 30 min, and **(F)** 38 min after injection. **G–L** The first 100 ms of positions are shown after each of several hundred randomly directed saccades, computed from the same data as **A–F**. Larger data points demarcate the last position of each 100-ms sequence. Animal: BAR

of eye position during an experiment in which muscimol was injected directly into the left INC. The vertical axis plots vertical eye position, whereas the horizontal axis plots clockwise (CW) and counterclockwise (CCW) rotation of the eye relative to primary position. The origin is the primary position defined by Listing's law, which in this animal is near the top of the position range. The upper row (A–D) shows the range of stable eye positions, i.e. positions for which velocity of torsional and vertical drift had dropped below a threshold of 2.5°/s. Before muscimol injection (A), almost all positions between saccades were stable, spread across a large (~70°) vertical range and a narrow (~3°) torsional range. Thus, these positions formed a plane (Listing's plane) that is viewed edge on. In the first 100 s after muscimol injection (Fig. 1 B) the eye began to settle at positions shifted clockwise from Listing's plane (one can visualize this as rotation of the tops of the monkey's eyes towards its right shoulder and the bottoms of its eyes towards its left shoulder). Simultaneously, the range of stable vertical positions began to diminish. For example, after 14 min (Fig. 1C) the vertical range was clearly restricted, particularly for downward gaze directions. At this time the torsional range was shifted by 10–15° CW, i.e. the eyes were rotated clockwise at all gaze directions. The final range of stable eye positions after 23 min (Fig. 1 D) was further reduced in the vertical direction.

How does initial post-saccadic eye position influence rate and direction of drift? The lower row of Fig. 1 (E–H) shows the first 100 ms of drift for various initial post-saccadic positions. The last position of each 100-ms sequence is given a larger symbol to indicate the direction of drift. As the vertical range of stable positions diminished (A–D), the magnitude of vertical drift (i.e. length of the 100-ms sequences) increased (E–H). This post-saccadic drift often exhibited a curved trajectory (e.g. Fig. 1 G), reflecting the fact that time constants of torsional drift tended to be slightly smaller than those of vertical drift (Crawford et al. 1991). The direction of vertical drift was upward or downward, depending on whether the saccade terminated below or above the range of stability. Since the final range of stable positions was in the upper part of oculomotor range (C–D), upward drift dominated (G–H). Similarly, the direction of torsional drift in Fig. 1 was clockwise (F), bidirectional (G), or counterclockwise (H), depending on the torsional end point of the saccades[1]

[1] Immediately after injection of muscimol into the left INC (e.g. Fig. 1 F) the saccades that followed each sequence of drift returned the eye towards the normal Listing's plane of zero torsion. Since it progressed towards a clockwise resting point, the direction of drift was always clockwise. However, later in the deficit (Fig. 1 G, H), saccades drove the torsional eye position progressively further clockwise away from Listing's plane towards and even beyond the range of stable torsional positions. Since the eye still drifted towards the same range, the direction of drift was then reversed (counterclockwise). Typically after injection of muscimol into either side of the INC, ocular drift was the first observed effect, and then after 0–30 min anti-corrective torsional saccades appeared. Similar torsional saccades have been observed after injections of muscimol 1–3 mm anterior to the INC, in the region of the riMLF saccadic burst neurons (Crawford and Vilis 1992). Injections of muscimol into the posterior riMLF produced this saccade deficit immediately and then afterwards produced positional drift similar to that seen in Fig. 1 H, perhaps due to spread of muscimol to the INC. Similarly, the appearance of anti-corrective torsional saccades, e.g. in Fig. 1 (G–H) was probably due to spread of muscimol from the INC to the riMLF on the same side. Injections placed between the INC and riMLF produced simultaneous drift and saccade deficits.

A second example (Fig. 2) shows the effects of injection on the right side of the brain. In this case, muscimol was injected just outside the anterior-lateral pole of the right INC, which resulted in a more gradual progression of the deficit. As with left INC injections, a thin range of stable torsional positions appeared, but now on the counterclockwise (CCW) side of Listing's plane, in this case stabilizing within 19 min (C). The range of vertically stable positions began to decrease with the first signs of positional drift (B), and then decreased progressively (B–F), presumably as muscimol diffused through the INC, until it finally approximated a point (F).

Figure 3 summarizes the final ranges of stable eye positions (e.g. Figs. 1 D, 2 F) from all experiments that produced severe post-saccadic drift. Part A gives the mean torsional and vertical value and standard deviations of positions within the final range of stability of one representative left and right INC inactivation from each animal. The torsional component of this range was shifted, but its standard deviation remained relatively small, i.e. the eyes were rotated torsionally from the normal zero value by about the same amount for all gaze directions. Although the vertical range was greatly reduced compared to normal (~70°), it typically retained a finite value of ~7°–14°. The mean values of the ranges of stability (e.g. those in Fig. 3 A) from all experiments with severe drift were further averaged across each animal to produce Fig. 3 B. The torsional range of stability was consistently shifted clockwise from the normal Listing's plane of zero torsion after left INC inactivation (○, △, ×, ○, □) and counterclockwise after right inactivation (▲, ■, ●). The average vertical component of this range was variable, but tended to cluster between an arbitrarily defined straight ahead position and the primary position defined by Listing's law (the origin of Fig. 3), which was rotated ~25° upward from straight ahead in these animals.

Why did this drift stabilize over such a relatively large range of vertical positions? As mentioned in the Introduction, the parallel integrator scheme predicts retention of a finite range of position stability during partial damage, whereas a single integrator scheme predicts a unique resting position (if an infinitely small velocity threshold were used). With a vertical velocity threshold of 1°/s as a practical lower limit, exponential leak of a single integrator predicts a very narrow null range (2 × threshold × time constant)° (Cannon and Robinson 1987). With a single integrator leaking with a time constant of 0.5 s, the above equation predicts that eye velocity will fall below 1°/s only within a range of less than one 1°. This velocity threshold (1°/s) was applied to data from five experiments (one from each animal) where time constants of simple exponential curves fit to the drift were less than 0.5 s (Crawford et al. 1991). The actual ranges of positions (farthest upward extent–farthest downward) that held at this threshold varied between 7.4° and 27.0°. The next section examines the factors that contribute to these relatively large ranges of eye stability.

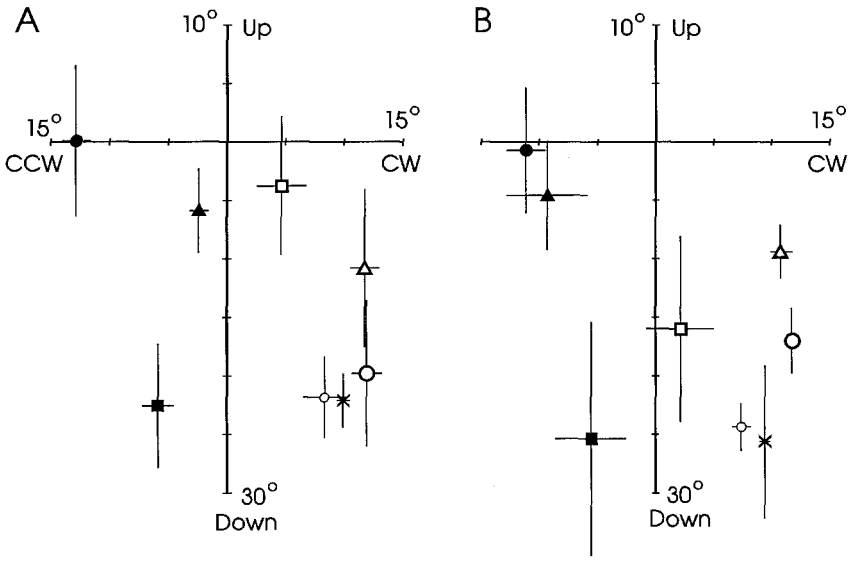

Fig. 3A,B. Summary of the torsional-vertical ranges of stable eye positions observed during unilateral inactivation of the interstitial nucleus of Cajal (INC) in all animals. Torsional position is plotted as a function of vertical position in Listing's coordinates, i.e. the vertical axis is embedded in Listing's plane and the origin is primary position. Eye position holding is defined as periods during which eye speed was less than 2.5°/s, as in Figs. 2–3. **A** Means and standard deviations for the range of torsional and vertical eye positions that held following representative INC inactivations from each animal. Data from the last file recorded were used. Key with animal code and N values (no. eye positions that held) for left INC inactivation: (○: CAS, 331 △: ART 270 x: LAR, 258 ○: MAR, 152 □: BAR, 33) and for right INC inactivation: (▲: ART, 233 ■: BAR, 148 ●: CAS, 42). **B** Averages and standard deviations (between experiments) of "stability range" means, as illustrated above, calculated from all unilateral experiments that resulted in severe positional drift. Means of ranges of stable vertical positions that retained a value greater than 50% of the normal position range were deemed imprecise and therefore not included (20% of the experiments). Key with animal code and N values (no. experiments) for left INC inactivation: (○: CAS, 2 △: ART, 4 x: LAR, 3 ○: MAR, 3 □: BAR, 5) and for right INC inactivation: (▲: ART, 5 ■: BAR, 6 ●: CAS, 4)

Determinants of vertical drift rate

If the neural network for velocity-to-position integration is equivalent to a single integrator circuit, then damage to this structure should result in a simple exponential drift that is proportional to eccentricity of eye position. During mild deficits, drift with a long time constant is expected, which would appear to be almost linear (Straube et al. 1991). However, the drift observed here did not follow this simple pattern. This is illustrated in Fig. 4, which shows a number of post-saccadic intervals starting at various vertical positions. The initial post-saccadic positions are aligned to the left. In the normal pre-injection state (A_1) the eye held steady at all levels of vertical position. Immediately after injection (A_2) vertical drift appeared, but there was no clear-cut relationship between eye position and the magnitude of the drift. At any one vertical level there was a mixture of positions that held and others that exhibited post-saccadic drift. After 9 min (A_3) a centripetal drift was more prominent at extreme vertical positions However, for intermediate vertical positions, different rates and directions of drift were observed at any one position. Furthermore, examination of individual sequences of drift did not reveal the almost linear segments that should be observed for small segments of drift with a long time constant. Instead, most of these sequences had a rapid initial rate of drift that often settled within 0.5 s.

One possibility was that a visual mechanism was intermittently stabilizing the drift. For example, Straube et al. (1991) have observed an increase in the range of stable horizontal positions in the light compared to the dark during muscimol inactivation of the horizontal integrator. However, the drift characteristics described above did not appear to depend on vision. Figure 4 B illustrates an example with similar pre-injection (B_1) and post-injection (B_2) data during spontaneous saccades in the dark. Again, the rate of drift did not correlate well with position, and the drift appeared to settle towards multiple resting points.

Eye-position drift began to approximate a simple position dependent exponent only after a considerable post-injection interval, e.g. 38 min in Fig. 4 C, at least from a superficial examination. In these cases there was a rapid centripetal (towards centre) vertical drift with a rate that appeared to be determined by eccentricity of eye position.

Contrary to the predictions of a single integrator model, post-saccadic drift often appeared to have more than one time constant. Multiple time constants were difficult to quantify in the absence of a single, unique resting position. However, this effect can be demonstrated qualitatively (Fig. 5). Figure 5 A shows several examples of downward saccades towards a position that was still above the central range of stability. In these cases, there was an initial segment of rapid post-saccadic drift in the direction opposite to the previous saccade, which then reversed direction and drifted more slowly towards centre. Figure 5 B shows two downward saccades away from the centre. Ideal exponential curves with one time constant (‴) have been fitted to the initial component of the upward post-saccadic drift. The real drift initially aligned with the ideal exponent, but then diverged and followed an almost linear path. In both A and B the initial segments of fast drift are in the direction opposite to that of the preceding saccade, while the final direction of slow drift was towards centre. Thus, there were at least two time constants of drift present. Furthermore, the shorter one appeared to be linked to the previous saccade, and the longer one appeared to be linked to current eye position.

Recall that a single integrator model predicts drift that is a simple function of current eye position and that this simple relationship was not observed in the data (Fig. 4) The observed irregularities appeared to be caused by an additional saccade dependence in the drift, as described

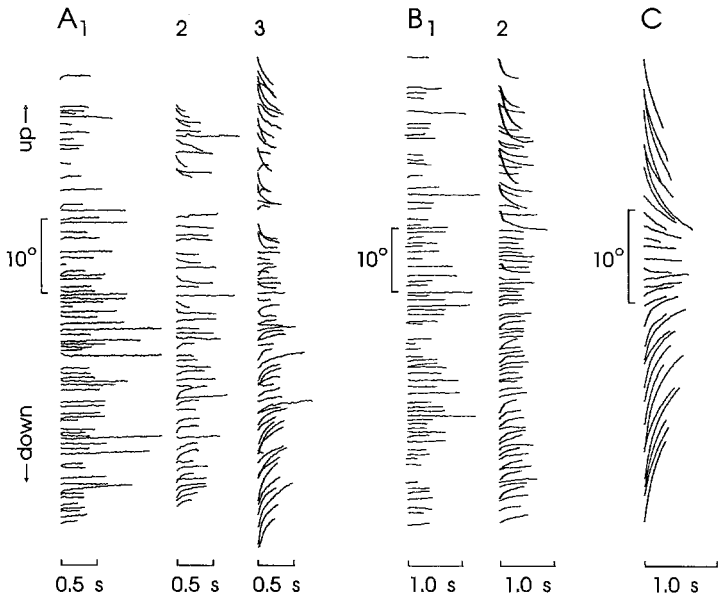

Fig. 4A–C. Vertical eye position (plotted as a function of time) after injection of muscimol into the interstitial nucleus of Cajal. Inter-saccadic intervals at various vertical levels are shown, aligned by left justification. **A** Typical injection effects in the light, showing position (*1*) before, (*2*) immediately after, and (*3*) 9 min after injection. Animal: CAS. **B** Positional drift during spontaneous saccades in the dark, (*1*) before, and (*2*) 3 min after injection. Animal: BAR. **C** 38 min after muscimol injection in BAR, in the light

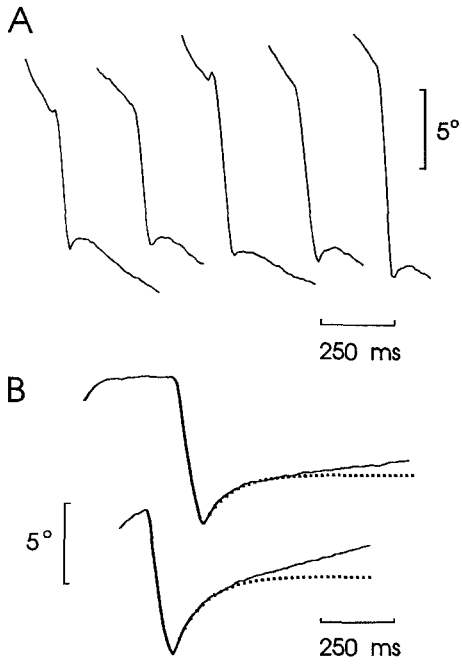

Fig. 5A,B. Multiple time constants in post-injection vertical position drift. **A** Five downward saccades starting near the upward edge of the position range and ending still above the central range of stable positions. Each saccade is preceded by downward drift, and is immediately followed by a brief but rapid drift that then reverses direction and slowly drifts downward towards the range of stable resting positions. **B** Two downward saccades, plotted on the same position scale, which started below the centre of the range of stability. A simulated segment of drift with a single 100–ms time constant (‴) has been fit to the initial portion of the post-saccadic drift. Animal: ART

above. Figure 6 A–D illustrates drift recorded in the dark as a function of the previous saccade. Vertical eye position is plotted against time for saccades converging on four different vertical levels. At any one of these levels, the size of the post-saccadic vertical drift appeared to be correlated to the vertical component of the previous saccade. For example, at 2° above primary position (A) the magnitude of downward post-saccadic drift increased with the magnitude of the previous upward saccade. At intermediate vertical levels (B), the direction of post saccadic drift reversed, depending on the direction of the previous saccade. In these respects, and in the rapid settling of the post saccadic drift, this resembled the phenomena known as pulse-step mismatch, a mismatch between the gains of oculomotor commands for movement and position holding.

In another respect the drift did not resemble a pulse-step mismatch. The drift was also dependent on eye position. Going downward in the position range from Fig. 6 A–D, there is a change in weighting from downward to upward drift. This is better illustrated by saccades with *similar* vertical magnitudes that terminated at different vertical positions (Fig. 6 E). The gradual transition from the lowest to highest saccade was accompanied by a transition from upward to downward drift.

If the magnitude and final resting position of post-saccadic drift is in part dependent on magnitude of the previous saccade, then steady fixation should be achieved by a succession of progressively smaller saccades to one target. Such was the case during mild initial post-injection effects. In Fig. 7 A, the animal made a series of downward saccades with similar end-points. The magnitude of post-saccadic drift decreased after each of the progressively smaller saccades. However, such stabilization did not occur beyond the progressively decreasing ranges illustrated in Figs. 1–3. For example, when the deficit shown in Fig. 7 had progressed further (B), there is no sign of stabilization after the nine downward saccades illustrated, nor indeed over the next 10 s of similar saccades (not illustrated). Thus, this inability to hold any eye position beyond an ever-narrowing central region, ultimately limited the range of stable eye positions.

Figure 8 quantifies the relations between vertical sac-

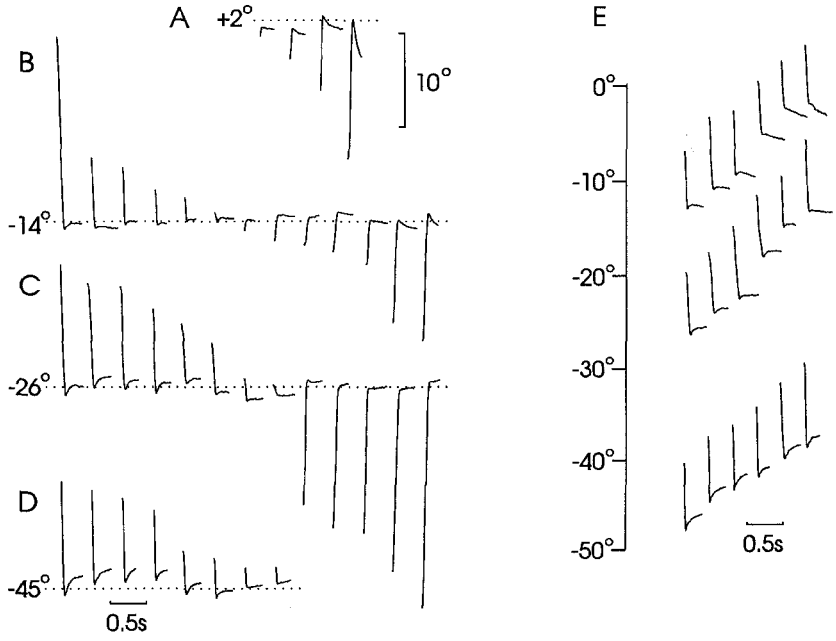

Fig. 6A–E. Dependence of vertical drift both on vertical eye position and vertical magnitude of the previous saccade. Data were recorded while the animal spontaneously made saccades in the dark. Vertical eye position is plotted against time. **A–D** Saccades with different magnitudes and directions, but with the same end point (‴), at four vertical levels. **E** Saccades with similar magnitudes, but different final positions. The choice of alignment is for conservation of space. Animal: BAR

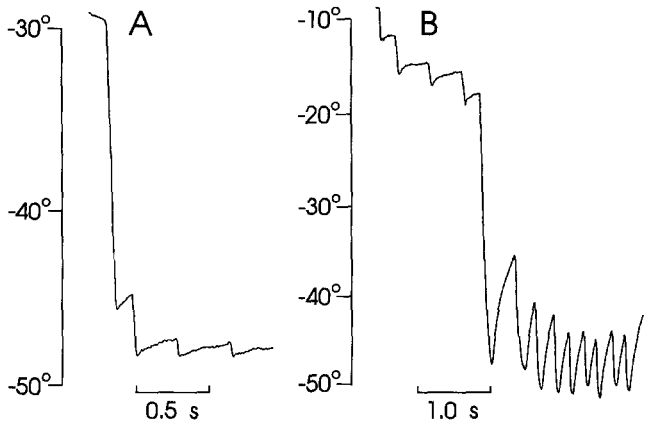

Fig. 7A,B. Eye-position drift following a series of saccades to the same eccentric vertical position. **A** Vertical position as a function of time during the initial effects of muscimol injection. **B** After further progression of the deficit. Animal: ART

cade magnitude, initial post-saccadic vertical eye position, and vertical drift. Drift magnitude was quantified as the vertical position change in the first 100 ms of post-saccadic drift. Figure 8 A plots drift magnitude (D) from one experiment as a function of initial post-saccadic position (P) on the left side, and as a function of previous saccade magnitude (S) on the right side. Standard statistical analysis (between two variables at a time) showed the expected correlation between drift magnitude and both position (e.g. $r = -0.971$ in the illustrated case) and saccade magnitude (e.g. $r = -0.842$). However, this is clearly a three-way problem in the abstract three-dimensional space defined by drift (D), position (P), and saccade magnitude (S). In particular, P and S were always correlated (e.g. $r = 0.765$, in the illustrated case), which could influence the two-dimensional results. Therefore a multiple-regression analysis was performed (Bevington 1969), which utilized the above correlation coefficients and a plane fit to the data points in the three-dimensional space of D, P, and S. This revealed that the data fell within a planar distribution. In Fig. 8 B, the data and axes from A have been rotated so that this plane is viewed edge-on, revealing the narrow orthogonal variance from this perspective. The multiple correlation coefficient (R) fit to this data was 0.983. This R, and all others computed from experiments in the light and dark, was significant far below the 1% level of error. This indicates that both independent variables P (position) and S (saccade magnitude) were required to explain the distribution of the dependent variable D (drift magnitude) (Bevington 1969).

Figure 8 C summarizes the statistical analysis from all animals. Bars give average statistical values for the initial effects of muscimol injection into the INC (hatched bars), and the last-recorded effects (solid bars). Standard two-way correlation coefficients (r) are shown for the relationship between eye position and drift magnitude (r[pd]), between saccade and drift magnitudes (r[sd]), and between the two independent variables, position and saccade magnitude (r[ps]). The three-way multiple regression analysis gave the slopes (m) of drift versus position for a constant saccade size (m[pd]), and drift versus saccade

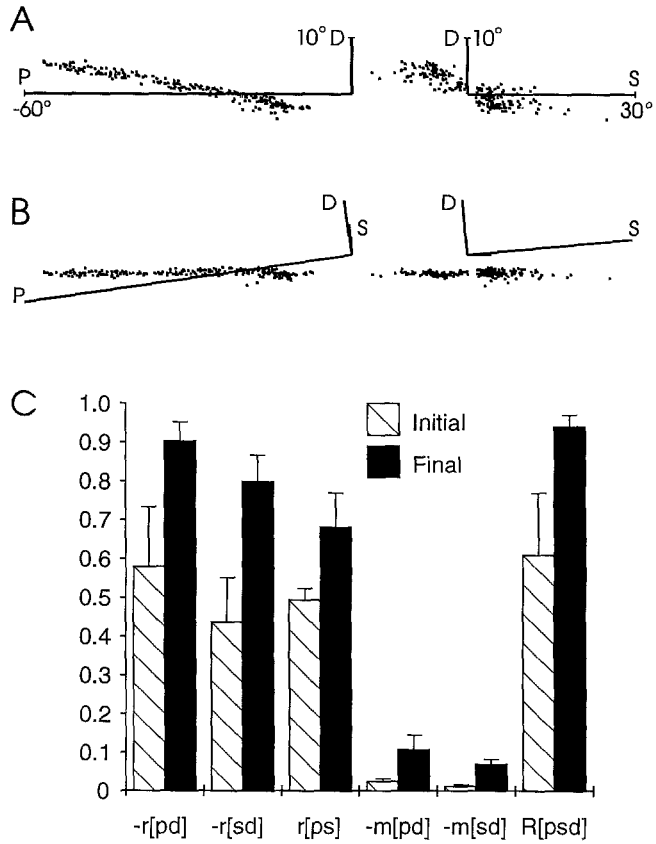

Fig. 8A–C. Statistical analysis of the relationship between drift, position, and saccades. **A** Magnitude of post-saccadic vertical eye position drift (D) in 100 ms plotted as a function of the initial post-saccadic vertical eye position (P) and of the vertical magnitude of the previous saccade (S). The data are viewed orthogonally to the coordinate axes from two views. $N = 230$. Animal: BAR. **B** The same data and coordinate axes have been rotated so that the planar distribution of data is viewed edge on. **C** Summary of a multiple regression analysis between D, P, and S in all animals. Initial and finally recorded data were analysed for a typical experiment from each animal. *Bars* illustrate the averages across all animals. Plotted are the average correlation coefficients between position and drift (r[pd]), average correlations between saccade magnitude and drift (r[sd]), average correlations between position and saccade magnitude (r[ps]), the average "slopes" of the former two relationships (m[pd] and m[sd]), and the average multiple correlation coefficients (R[psd]). Negative correlation coefficients have been reversed to conserve space, and *error bars* indicate the standard deviations of the values between animals

size for a constant position (m[sd]). Not surprisingly, these slopes became steeper between the initial and final measured effects, as drift magnitude increased. Finally, the average multiple correlation coefficients (R[psd]) were 0.610 for the initial effects (when slopes m[pd] and m[sd] were changing rapidly) and 0.941 for the final, more stable effects. The latter was clearly higher, suggesting almost all variability had been accounted for. However, all individual R values were significant ($P < 0.01$), even for drift which superficially appeared to show a simple position-dependence (e.g. Fig. 4 C). This quantitative analysis confirms that not only current eye position, but also previous saccadic history are necessary to account for the observed post-saccadic drift.

Discussion

Simulation of the data using single and parallel integrator models

As stated in the Introduction, the purpose of this investigation was not to develop a new model of the oculomotor integrator, but rather to test one fundamental principle incorporated into two previously described network models. Does the integrator react to damage like a network with uniformly distributed connections (Arnold and Robinson 1991) or like a network that utilizes a modular pattern of lateral connections (Cannon et al. 1983)? Our aim was to compare the data to two simple equivalent models that would illustrate the key features of these two configurations. Therefore, we developed a simple one-dimensional model of the brainstem saccade generator[2] that incorporated either a single integrator (Fig. 9 A), equivalent to the uniformly distributed network, or one in which integration was distributed across a parallel array of integrators (Fig. 9 B), equivalent to the modular network. The latter model utilized a number (n) of simple integrators, each receiving a copy of the burst neuron velocity signal and contributing $1/n$ of the position signal to motoneurons. Ten parallel integrators were used in the simulations illustrated below. This concept is the same as that used by Abel et al. (1978), who used two parallel integrators to simulate partial integrator failure. Progressive disruption to a single neural integrator was simulated by causing an integrator (Fig. 9 A) to leak with progressively lower time constants. The effect of muscimol spreading through parallel neural integrators in the INC was simulated by inactivating an increasing number of local integrators (Fig. 9 B) and introducing leak in an increasing number of adjacent integrators.

Figure 10 illustrates the essential differences between simulated damage to the two integrator models. When the eye position signal was generated by a single leaky integrator (Fig. 10 A), position always drifted towards a unique resting position (– – –), at a rate determined uniquely by current eye position. Finite segments of slower drift appeared to be almost linear. However, the drift

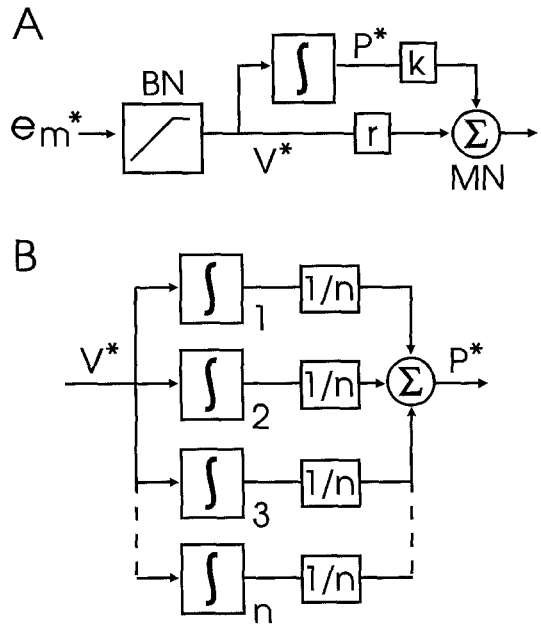

Fig. 9. Models of the brainstem saccade generator incorporating a single velocity-to-position integrator (**A**), and multiple parallel integrators (**B**). **A** Main elements of the saccade generator. *Asterisks* denote internal kinematic representations. Current motor error (e_{m*}) was converted to a velocity command (V^*) by a saturating gain element, the burst neurons (*BN*). V^* was then sent directly to the motoneurons (*MN*) and to a positive feedback integrator that provided the position signal (P^*). The sum of V^* and P^* were input to a standard 1-D plant model (not shown), with viscosity constant (r) and elasticity constant (k) set at 1 and 5, respectively, giving an intrinsic plant time constant of 200 ms (Robinson 1970, 1975). e_{m*} is the difference between desired displacement (desired – current position) and displacement feedback that is derived upstream from the main integrator (Jürgens et al. 1981). **B** Parallel array of n integrators used to replace the single integrator in **A**. Each integrator contributes $1/n$ of the position signal to the motoneurons. Integration was performed during each simulated 1 ms iteration in the program as follows: $P^*new = (1\text{–leak}) \times (P^*old + \triangle t \times V^*)$, where P^*new and P^*old are the position signals generated by the integrator at the current and previous moments, and $\triangle t$ is the time interval between these moments. The term "leak" is a variable that was varied between zero (perfect integration) and one (complete inactivation)

was exponential with a single time constant. This was primarily determined by the time constant of the leaky integrator, until this became small compared to the time constant of the oculomotor plant, which set the lower limit.

As expected, the parallel integrator model produced more complex effects. This model gave an effect equivalent to a pulse-step mismatch when some integrators were intact and others were completely inactive (Fig. 10 B). For example, if 30% of the integrators were completely inactivated each saccade was followed by a reversing drift with the time constant of the plant, towards a position 30% of the way back to the start. This final resting position (– – –) then held indefinitely. Thus, there was no longer a unique resting position, but rather brief, rapid drift towards multiple resting positions. As long as the eye was allowed to settle between saccades, post-saccadic drift was determined uniquely by the magnitude and direction of the previous saccade, rather than eye position.

[2] When simulating neural integrator failure, it is important to know how this will affect saccade generation. Saccade metrics could be affected for two reasons. First, the integrator could lie within a neural feedback loop that guides and terminates saccades. If the integrator is in the feedback loop proposed by Robinson (1975), then integrator failure should cause saccade overshoot. However, saccades undershot slightly during inactivation of the horizontal integrator (Kaneko and Fuchs 1991) or the vertical integrator (Crawford et al. 1988) in trained monkeys. Therefore, the integrator appears to be downstream from the feedback loop that guides saccades (Jürgens et al. 1981), as in our model. Second, most neurons in the integrator region carry a saccade-related burst signal as well as a position signal and such a burst could contribute to saccade generation if it reaches the motoneurons. However, a recent study suggests that only the position-related cells without the burst are the true output neurons of the integrator (Escudero et al. 1992). Furthermore, the slight saccadic undershoots observed during integrator failure were simulated by our model simply by reducing the position signal, without affecting the eye-velocity command. Thus, the use of a pure position signal in our model's integrator pathway appears to be justified for the purpose of this study.

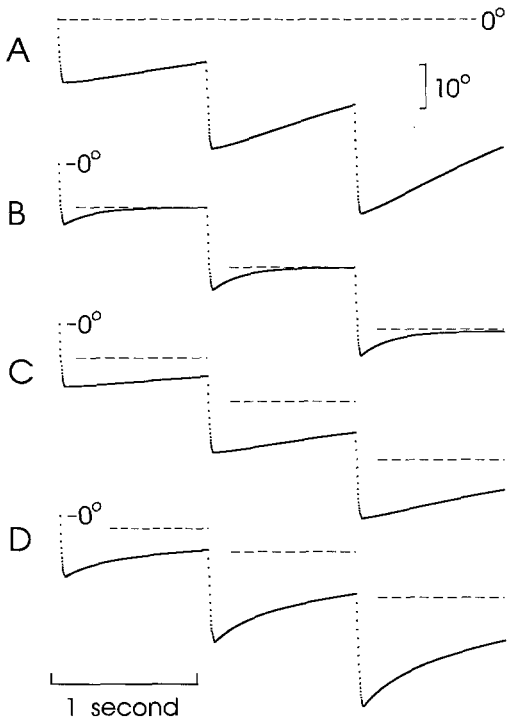

Fig. 10. Theoretical relationships between saccade magnitude, eye position, and drift using the single integrator model (**A**) and the multiple integrator model (**B–D**). Simulated vertical eye position is plotted (at 2-ms intervals) as a function of time. In each case the eye is initialized at the zero position and then makes three saccades towards targets 15°, then 30°, then 45° down at intervals of 1 s. (– – –): The current resting position that position settles towards. **A** Position signal generated by a single integrator that leaks with a time constant of 2 s. **B** Position signal generated by ten parallel integrators, of which 30% were completely inactivated. **C** 50% of the parallel integrators leaking with a time constant of 2 s. **D** A combination of **B** + **C**, i.e. 30% of the integrators were inactivated, 50% leaked with a 2-s time constant, and 20% remained intact

The parallel integrator model did not produce a simple pulse-step mismatch when the time constant of integrator leak was long compared to the inter-saccadic interval. Figure 10 C illustrates this with 50% of the integrators leaking with a 2-s time constant, the same as that used in 10 A. At the second saccade, the leaky integrators still maintain some neural activity from the first saccade, and similarly they maintain activity from the previous two saccades at the third saccade. However, unlike the case of the leaky single integrator, when saccades suddenly ceased, eye position did not settle to a unique resting position, but rather to a value determined by activity in the intact integrators (– – –).

Finally, if some integrators leak rapidly, others slowly, and others not at all, (Fig. 10 D), one observes a combination of the position-related and saccade-related effects illustrated in B and C. The drift still had multiple resting positions. Moreover, this drift had more than one time constant, with the rapid drift correlated more to the saccade (for reasons discussed above) and the slow drift correlated more to current position. Thus, this model simulates three features of the experimentally observed drift that could not be accounted for by a single leaky integrator: multiple resting positions (Figs. 1–7), multiple time constants (Fig. 5), and dependence of drift rate on the previous saccadic history as well as current eye position (Figs. 6–8). These three observations show that the single time constants and resting positions used previously to quantify integrator failure do not adequately describe the deficit (Cannon and Robinson 1987; Cheron and Godaux 1987; Fukushima 1987; Crawford et al. 1991; Straube et al. 1992)[3]

Rebound nystagmus, integrator saturation, and the range of stable resting positions

Rebound nystagmus is a condition characterized by a progressive decrement in drift towards centre during a series of eccentric saccades (Fig. 7 A), and then a drift away from centre after the subsequent saccade towards centre (Fig. 5 A) (Leigh and Zee 1991). Rebound nystagmus has been reported during recovery from damage to the integrator for horizontal eye position (Cannon and Robinson 1987) and in cerebellum-damaged patients (Bondar et al. 1984), as well as in the present investigation.

This deficit results from an imbalance between the gains of the movement command and the position command (pulse-step mismatch). Inactivation of a fraction of parallel sub-integrators is one possible substrate for this imbalance. Whereas a single leaky integrator cannot simulate rebound nystagmus after a saccade towards centre (Fig. 11 A), this is an inherent prediction of the parallel integrator model (Fig. 11 B). The parallel model also simulates the subsequent reversal of drift direction towards centre observed in Fig. 5 A. Drift is dominated first by the faster, more saccade-dependent drift, and then by the slower, seemingly position-dependent drift. This model suggests that at least one mechanism for rebound nystagmus depends on the function of intact parts of the integrator, as suggested previously (Cannon and Robinson 1987; Leigh and Zee 1991).

[3] Manipulations of the single integrator model can simulate some of our results, but this model still fails for fundamental reasons. Post-saccadic drift can be simulated by two means with a single integrator: (1) reducing the gain of saccade velocity input to the integrator produces a pulse-step mismatch with saccade-related drift and (2) reducing the gain of the positive feedback loop that maintains integrator activity produces a leaky integrator and position-dependent drift. In the illustrated simulations, both gains were equally reduced to simulate post-synaptic inhibition, but the integrating positive feedback loop was so much more sensitive that the position-dependent drift completely dominated. By adding a much greater pulse-step mismatch (decreasing input gain to the integrator by 1000 times the decrease in feedback gain), the model was able to simulate a combined position-dependent and saccade-dependent drift like the data. However, this model still failed to maintain eye positions at multiple resting positions, because the single integrator will always leak to zero activity. In order to simulate the multiple, saccade-related resting positions observed in the data, there must be a different DC bias in the integrator pathway after each saccade. Such a saccade-dependent bias implies that there is a functional integrator that receives saccadic input in parallel to the non-functional integrator. This is exactly what occurs in our parallel integrator model.

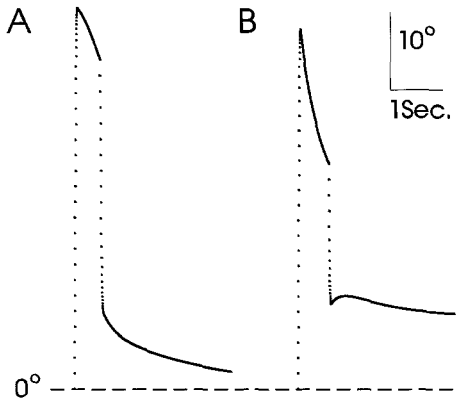

Fig. 11. Simulations of rebound nystagmus and reversal of drift direction. Eye position is plotted (at 4–ms intervals) as a function of time. **A** Position signal generated by a single integrator leaking with a 2–s time constant. **B** Position signal generated by 10 parallel integrators of which 30% were completely inactivated, 40% leaked with a 1–s time constant, and 30% were intact. In each case the model was programmed first to produce a saccade upwards from zero towards 50° up, and then after 600 ms a saccade downwards towards a position 10° up from zero

The presence of intact integrators is particularly important for stabilization of gaze after a series of saccades to the same target. With a single leaky integrator model there is no opportunity to stabilize gaze, for example at 20° or 40° down (Fig. 12 A). With 20% of the parallel integrators completely inactivated and 30% leaking with various time constants (100, 200, and 500 ms), simulated eye position stabilized within ~3 s (Fig. 12 B). This stabilization occurred because the intact integrators "charged up", while the damaged integrators stabilized towards zero activity.

In the experimental data, animals could not use this strategy to stabilize gaze beyond some progressively decreasing range of stable eye positions (Fig. 7 B). The model used in Fig. 12 B failed to show this behaviour because its intact integrators, unlike real neurons, were allowed to charge up indefinitely. Figure 12 C shows the effect of adding a more realistic saturation. The simulated integrator neurons were limited to fire within a 500 Hz range, corresponding to an eye-position range of ±50°. With such a saturation, the intact neurons (50% of the total) could only maintain a maximal total position signal of ±25°. Therefore, the series of saccades towards 20° down are unaffected by this saturation, but eye position can no longer be stabilized at 40° down, no matter how many saccades occur. Figure 12 D uses the same saturating model, but now only 20% of the integrators are intact, increasing the magnitude of drift and further limiting the maximal range of eye stabilization to ±10°. Thus, both the percentage of intact integrator units and their saturation limit ultimately determine the range of stable resting positions.

If we assume that integrators normally saturate near the boundary of the oculomotor range, as simulated above, then the fraction of intact integrator units could be estimated by taking the ratio between the range of stable resting eye positions in the affected subject, and the same range in the normal subject (range of stable positions/normal oculomotor range). The assumption that integrator activity saturates at the oculomotor range is supported by our observation that the range of stable positions began to decrease with the first signs of ocular drift. It is also supported by the rapid increase in drift velocity observed near the oculomotor limits of normal humans (end point nystagmus), particularly under fatiguing conditions that might reduce the saturation point (Eizenman et al. 1990). Such boundary saturation would confer a useful safety feature to the oculomotor system: eccentric eye movements, such as an uninterrupted VOR slow phase, would be prevented from over-charging the integrator to represent positions beyond the plant's me-

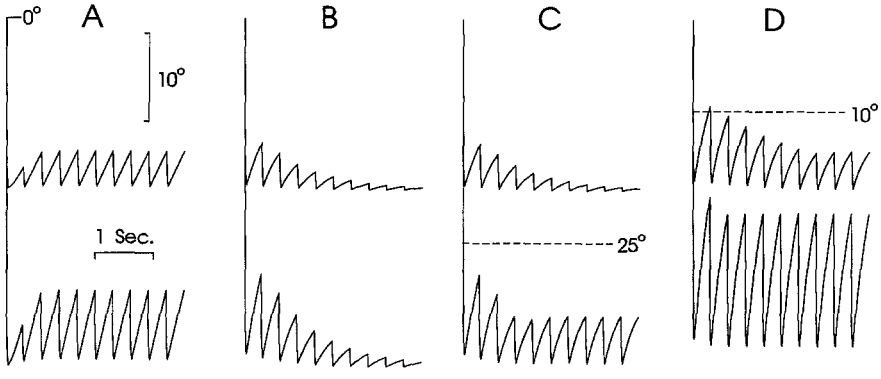

Fig. 12. Vertical nystagmus patterns using the single (**A**) and multiple integrator model (**B–D**). Simulated eye positions are initialized to zero and then plotted during 3 s of saccades occurring at intervals of 300 ms. In each case a series of saccades directed towards 20° down is superimposed over a second series towards 40° down. **A** Position signal generated by a single integrator which leaks with a time constant of 1 s. **B** Position signal generated by ten parallel integrators of which 50% were intact, 20% were completely inactivated, and the other three leaked with various time constants (100, 200, 500 ms). **C** Same as previous simulation, except that the integrating tonic neurons were given a saturation at ±250 Hz (normally corresponding to 50° eccentricity using simulated neurons with a position sensitivity of five spikes/s per degree). In a network model in which neurons modulate their activity up and down about a baseline, this saturation would correspond to a lower limit of zero and an upper limit of 500 spikes per second. **D** As in previous simulation, except that three additional integrators have been inactivated. The horizontal lines (– – –) in **C** and **D** indicate the maximal eccentricity of eye position that can be maintained by the intact integrators

chanical range. In general, such position signal saturation would be a useful safety feature for any motor system. First, muscles could not be inefficiently and dangerously driven against an unyielding mechanical limit in their range. Second, efference copies of body position (perhaps derived from neural integrators) are thought to be used for programming movements (Robinson 1975; Jürgens et al. 1981); integrator saturation would prevent transmission of erroneous representations of positions that are beyond the system's mechanical range.

Anatomical organization of the network

The oculomotor velocity-to-position transformation is thought to be distributed between several interdependent brainstem nuclei (King and Leigh 1982; Cannon and Robinson 1987; Cheron and Godaux 1987; Fukushima 1987; Tweed and Vilis 1987). If our above discussion is correct (fraction of intact integrator units = range of stability/oculomotor range), then our data suggest that 10–50% of the vertical integrators were unaffected by unilateral muscimol injections. These intact integrators may have resided in unaffected parts of the INC or in other nuclei. Torsional ranges of stability were consistently narrow (Fig. 3 A), and torsional drift was more rapid than vertical drift during INC inactivation (Crawford et al. 1991). This suggests that torsional integration is even more sensitive to INC damage than vertical integration.

The observation that unilateral INC inactivation abolished both clockwise and counterclockwise position holding supports the view that the two sides of the integrator are interdependent (Cannon et al. 1983; Galiana and Outerbridge 1984: Cannon and Robinson 1987; Anastasio and Robinson 1991). Despite this interdependence, their inputs appear to be symmetrically opposite, receiving inputs from the contralateral semicircular canals (Fukushima et al. 1990). In agreement with this, stimulation of the left nucleus prepositus hypoglossi produces leftward eye movements, while stimulation of the right prepositus produces rightward eye movements (Cannon and Robinson 1987). Similarly, stimulation of the left INC produces CCW movements, whereas right INC stimulation produces CW eye rotations (Crawford et al. 1991). Moreover, Injection of muscimol into these same sites produces eye drift towards resting points shifted in the opposite directions: after unilateral injection into the nucleus prepositus hypoglossi the eyes drifted away from the side of the injection (Yokota et al. 1992), and in the present study, injection into the right and left INC produced drift towards CCW and CW resting points, respectively. Similar torsional shifts were reported after unilateral inactivation of the INC in normal and labyrinthectomized cats (Anderson 1981; Fukushima et al. 1992). These shifts and concomitant torsional drift were also reported in humans with unilateral damage to the INC region (Halmagyi et al. 1990, Halmagyi and Hoyt 1991).

These results can be accounted for by the model of Cannon et al. (1983), who suggested a scheme with a bilateral, mutually inhibitory pair of neurons with opposite inputs (in this case with excitatory CCW inputs on the left and CW on the right). Inhibition of one side should disrupt both CW and CCW integration, and block transmission on that side. The remaining contralateral channel would allow background activity of integrator neurons and their inputs simply to pass through, and the unopposed net output would produce the observed shifts in the range of stable torsional positions (Anderson 1981; Fukushima et al. 1992).

Concluding remarks

The present investigation suggests that neural velocity-to-position integration is distributed across an array of parallel independent sub-integrators, which requires that lateral connections within the integrator network are restricted to a modular pattern. The advantages of this modularity for the oculomotor integrator include a relative immunity to microlesions and other random computational errors, maintenance of some fraction of function after more extensive damage, and potential for recovery through local parametric adjustments (Cannon et al. 1983). A similarly redundant mechanism would provide comparable advantages for many other neural computations. For example, modular retinotopic maps in the brain may be viewed as parallel arrays of computational units, each performing similar operations on a restricted segment of information. Local damage produces a small scotoma, whereas local damage to a fully distributed representation would produce degradation of the entire visual image. Such robustness may be one important consequence of the modular patterns of neural connectivity (e.g. cortical columns) observed throughout the brain (Mountcastle 1957; Hubel and Weisel 1959; Purves et al. 1992).

Acknowledgements. We gratefully acknowledge the technical assistance of Leopold Van Cleef, Sheila Nicol, Garth Santor, and Sherry Watts. We also thank Jon Hore and Doug Tweed for detailed commentaries on this manuscript. This study was supported by Medical Research Council of Canada Grant MT9335. Doug Crawford holds a Medical Research Council of Canada Fellowship.

References

Abel LA, Dell'Osso LF, Daroff RB (1978) Analog model for gaze-evoked nystagmus. IEEE Trans Biomed Eng 25:71–75

Anastasio TJ, Robinson DA (1991) Failure of the oculomotor neural integrator from a discrete midline lesion between the abducens nuclei in the monkey. Neurosci Lett 127:82–86

Anderson JH (1981) Ocular torsion in the cat after lesions of the interstitial nucleus of Cajal. Ann NY Acad Sci 374:865–871

Anderson JH, Precht W, Papas C (1979) Changes in the vertical vestibuloocular reflex due to kainic acid lesions of the interstitial nucleus of Cajal. Neurosci Lett 14:259–264

Arnold DB, Robinson DA (1991) A learning model of the neural integrator of the oculomotor system. Biol Cybern 64:447–454

Bevington PR (1969) Data reduction and error analysis for the physical sciences. McGraw-Hill, New York, pp 198–200

Bondar RL, Sharpe JA, Lewis AJ (1984) Rebound nystagmus in olivocerebellar degeneration: a clinicopathological correlation. Ann Neurol 15:474–477

Cannon SC, Robinson DA (1987) Loss of the neural integrator of the oculomotor system from brainstem lesions in the monkey. J Neurophysiol 57:1383–1409

Cannon SC, Robinson DA, Shamma S (1983) A proposed neural network for the integrator of the oculomotor system. Biol Cybern 49:127–136

Carpenter RHS (1972) Cerebellectomy and the transfer function of the vestibulo-ocular reflex in the decerebrate cat. Proc R Soc Lond [Biol] 181:353–374

Cheron G, Godaux G (1987) Disabling of the oculomotor integrator by kainic acid injections in the prepositus-vestibular complex of the cat. J Physiol (Lond) 394:267–290

Cohen B, Komatsuzaki A (1972) Eye movements induced by stimulation of the pontine reticular formation: evidence for integration in oculomotor pathways. Exp Neurol 36:101–117

Crawford JD, Cadera W, Vilis T (1988) The oculomotor velocity to position transformation involves the nucleus of Cajal. Soc Neurosci Abstr 14:386.8

Crawford JD, Cadera W, Vilis T (1991) Generation of torsional and vertical eye position signals by the interstitial nucleus of Cajal. Science 252:1551–1553

Crawford JD, Vilis T (1991) Axes of eye rotation and Listing's law during rotations of the head. J Neurophysiol 65:407–423

Crawford JD, Vilis T (1992) Symmetry of oculomotor burst neuron coordinates about Listing's plane. J Neurophysiol 68:432–448

Crick F (1989) The recent excitement about neural networks. Nature 337:129–132

Eizenman M, Cheng P, Sharpe JA, Frecker RC (1990) End-point nystagmus and ocular drift: an experimental and theoretical study. Vision Res 30:863–877

Escudero M, De La Cruz RR, Delgado-Garcia JM (1992) A physiological study of vestibular and prepositus hypoglossi neurones projecting to the abducens nucleus in the alert cat. J Physiol (Lond) 458:539–560

Fukushima K (1987) The interstitial nucleus of Cajal and its role in control of movements of head and eyes. Prog Neurobiol 29:107–192

Fukushima K, Harada C, Fukushima J, Suzuki Y (1990) Spatial properties of vertical eye movement-related neurons in the region of the interstitial nucleus of Cajal. Exp Brain Res 79:25–42

Fukushima K, Ohashi T, Fukushima J, Kase M (1992) Ocular torsion produced by unilateral chemical inactivation of the interstitial nucleus of Cajal in chronically labyrinthectomized cats. Neurosci Res 13:301–305

Galiana HL, Outerbridge JS (1984) A bilateral model for central neural pathways in vestibuloocular reflex. J Neurophysiol 51:210–241

Halmagyi GM, Brandt T, Dietrich M, Curthoys IS, Stark RJ, Hoyt WF (1990) Tonic contraversive ocular tilt reaction due to unilateral meso-diencephalic lesion. Neurology 40:1503–1509

Halmagyi GM, Hoyt WF (1991) See-saw nystagmus due to unilateral mesodiencephalic lesion. J Clin Neuro Ophthalmol 11:79–84

Helmholtz H (1925) Treatise on physiological optics. English translation by Southall JPC. Opt Soc Am, Rochester NY, pp 44–51

Hubel DH, Weisel TN (1959) Receptive fields of single neurones in the cat's striate cortex. J Physiol (Lond) 148:574–591

Jürgens R, Becker W, Kornhuber HH (1981) Natural and drug induced variations of velocity and duration of human saccadic eye movements: evidence for a control of the neural pulse generator by local feedback. Biol Cybern 39:87–96

Kamath BY, Keller EL (1976) A neurological integrator for the oculomotor control system. Math Biosci 30:341–352

Kaneko CRS, Fuchs AF (1991) Saccadic eye movement deficits following ibotenic acid lesions of the nuclei raphe interpositus and prepositus hypoglossi in the monkey. Acta Otolaryngol [Suppl] (Stockh) 481:213–215

King WM, Fuchs AF (1979) Reticular control of vertical saccadic eye movements by mesencephalic burst neurons. J Neurophysiol 42:861–876

King WM, Fuchs AF, Magnin M (1981) Vertical eye movement-related responses of neurons in midbrain near interstitial nucleus of Cajal. J Neurophysiol 46:549–562

King WM, Leigh RJ (1982) Physiology of vertical gaze. In: Lennerstrand G, Zee DS, Keller EL (eds) Physiology of vertical gaze in functional basis of ocular motility disorders. Pergamon Press, Oxford, pp 267–276

Leigh RJ, Zee DS (1991) The neurology of eye movements, 2nd edn. Contemporary neurology series. Davis, Philadelphia, pp 188–191

Mountcastle VB (1957) Modality and topographic properties of single neurons of cat's somatic sensory cortex. J Neurophysiol 20:408–434

Purves D, Riddle DR, La Mantia A-S (1992) Iterated patterns of brain circuitry (or how the cortex gets its spots). Trends Neurosci 15:362–368

Robinson DA (1968) Eye movement control in primates. Science 161:1219–1224

Robinson DA (1970) Oculomotor unit behaviour in the monkey. J Neurophysiol 33:393–404

Robinson DA (1974) The effect of cerebellectomy of the cats vestibulo-ocular integrator. Brain Res 71:195–207

Robinson DA (1975) Oculomotor control signals. In: Bach-y-Rita P, Lennerstrand G (eds) Basic mechanisms of ocular motility and their clinical implications. Wenner-Gren Cent Int Symp Ser. Pergamon, Oxford, pp 337–374

Rosen MJ (1972) A theoretical neural integrator. IEEE Trans Biomed Eng 19:362–367

Shantha TR, Manocha SL, Bourne GH (1968) A stereotaxic atlas of the java monkey brain. Karger, New York, pp 32

Straube A, Kurzan R, Büttner U (1991) Differential effects of bicuculline and muscimol microinjections into the vestibular nuclei on simian eye movements. Exp Brain Res 86:347–358

Tweed D, Cadera W, Vilis T (1990) Computing three-dimensional-eye position quaternions and eye velocity from search coil signals. Vision Res 30:97–110

Tweed D, Vilis T (1987) Implications of rotational kinematics for the oculomotor system in three dimensions. J Neurophysiol 58:832–849

Tweed D, Vilis T (1990) Geometric relations of eye position and velocity vectors during saccades. Vision Res 30:111–127

Westheimer G (1957) Kinematics of the eye. J Opt Soc Am 47:967–974

Yokota J, Reisine H, Cohen B (1992) Loss of integrator function after injection of GABAergic substances into the prepositus hypoglossi nuclei (PPH). Soc Neurosci Abstr 18:215.9